

Oligomer-to-Polymer Transition of Poly-(propylene glycol) Revealed by Dielectric Normal Modes

Catalin Gainaru* and Roland Böhmer

Fakultät für Physik, Technische Universität Dortmund,
44221 Dortmund, Germany

Received August 12, 2009

Revised Manuscript Received September 17, 2009

The oligomer-to-polymer transition of propylene glycol chains with $N = 13, \dots, 314$ repeat units is studied via dielectric normal modes. In the Gaussian regime the ratio of the dispersion strengths of the normal mode to that of the segmental mode (α -process) is expected to be independent of N . For poly-(propylene glycol) we find the onset of this regime at $N \approx 30$. This onset is, however, not accompanied by a breakdown of the Rouse model, which is expected in the short-chain limit. In that sense, static and dynamic properties reveal the oligomer-to-polymer transition at different molecular weights.

The dynamics of reasonably long polymer chains can be regarded as well understood in the nonentangled as well as in the entangled, molten state.¹ The question at which chain length polymer-specific properties emerge has been of interest for quite some time^{2–5} and is also recently receiving considerable attention.^{6,7} Polymer-specific properties are accounted for by the Rouse model or its refinements as soon as the chain conforms to Gaussian statistics, a feature well studied also using molecular dynamics simulations.⁸ A polymer is usually considered to be in the Gaussian regime if its contour or end-to-end distance obeys random walk statistics. However, the assessment of this regime on the basis of experimental data is still a matter of debate. Changes in the molecular weight dependence of the glass transition temperature or other dynamical properties were suggested as indicators for the onset of the polymer regime.⁹ However, the reliability of this approach was recently questioned, and the importance of static properties was emphasized.¹⁰

In the present article we exploit the direct access to the overall chain dynamics provided by polymers with a dipole moment along their contour. These so-called type A polymers give rise to a significant dielectric signature. This dipolar normal mode (NM) was mostly exploited to study the onset of entanglement effects with polyisoprene probably being the best studied example.^{11,12} For the present work we selected poly(propylene glycol) (PPG) for which the molecular weight dependence of the segmental dynamics has been well characterized.^{2,3,19} In particular, PPG served as a testing ground to clarify the mutual relation of α - and β -processes as a function of chain length.¹³

Propylene glycols from various sources were used, covering the range $770 \text{ g/mol} \leq M_w \leq 18\,200 \text{ g/mol}$.¹⁴ The corresponding number of constituent segments varies between $N = 13$ and $N = 314$. The polydispersity index M_w/M_n typically was 1.03 and for the longest chains was around 1.02. To enhance the visibility of the low-frequency flank of the normal mode, an electrical cleaning procedure¹⁵ was employed when needed to suppress the residual electrical conductivity by roughly a factor of 10.¹⁶

Figure 1 compiles dielectric loss $\epsilon''(\nu)$ data for a temperature $T = 245 \text{ K}$ at which both segmental and normal mode relaxations

are in the experimental window for the samples with $13 \leq N \leq 314$. One recognizes that all data exhibit the same global peak frequency because the segmental dynamics is largely unaffected by the chain length. To emphasize the relative strength of the normal mode peaks emerging for larger N , the data were normalized by $\epsilon''_{\text{peak},\alpha}$. In accord with previous observations,¹⁷ $\epsilon''_{\text{peak},\alpha}$ decreases by a factor of 2 when N is varied between 13 and 314. In Figure 1 the relative amplitudes of the normal mode peaks are seen to increase slightly with decreasing M_w . However, this does not imply that their dispersion strength depends on N because concomitantly with decreasing M_w the high-frequency flank of the NM peak also becomes steeper, as discussed next.

In order to quantify the spectral changes the data in Figure 1 were fitted using a sum of two Havriliak–Negami functions $\epsilon^* = \sum_{p=1,2} \Delta\epsilon_p [1 + (i2\pi\nu\tau_p)^{\alpha_p}]^{-\gamma_p}$, with $p = \{\alpha, \text{NM}\}$. The low- and high-frequency flanks of the relaxation peaks are given by $\epsilon'' \sim \nu^\alpha$ and $\epsilon'' \sim \nu^{-\alpha'}$, respectively. Their dispersion strengths are $\Delta\epsilon_p$, and the time constants are denoted as τ_p . The exponent α_{NM} was kept fixed to a value of 1 for all samples except $N = 93$. Here α_{NM} was close to 0.9, probably due to the slightly higher value of the polydispersity index for this particular sample (1.06). For $N \geq 35$ the α - and NM-processes are well separated (see Figure 1a), and the low-frequency exponent of the α -peak is easily accessed. The value for this exponent appears to be independent of N , i.e., $\alpha_\alpha = 0.88 \pm 0.03$. However, for $N < 35$ the two processes tend to merge (see Figure 1b) and free fits did not converge. In order to overcome this problem we assumed $\alpha_\alpha = 0.88$ to hold also for lower N (cf. the dashed line in Figure 1), and the fits represented as solid lines in Figure 1b for $N = 22, 17$, and 13 were obtained. These fits yielded the high-frequency exponent of the NM, γ_{NM} , which continuously increases with decreasing N for all systems under consideration. To check for systematic errors in the fitting procedure, the data were alternatively analyzed using the Williams–Watts product approach.¹⁸ The most important outcome of all these fitting procedures is that the static response of polymers with sufficiently large chain lengths is independent of N .

The relative relaxation strength of the NM with respect to that of the α -peak is shown in Figure 2a. It is seen that $\Delta\epsilon_{\text{NM}}/\Delta\epsilon_\alpha$ increases strongly starting from $N \approx 10$ as the normal modes gain weight, while for $N \geq 30$ this ratio is N -independent. In order to offer a different perspective on the transformation between the two regimes, in Figure 3 we present the step response functions $\phi(t)$ obtained by numerically transforming the data shown in Figure 1 into the time domain. In this representation the relative amplitude of the NM relaxation with respect to the α -process is directly given by the value of the plateau obvious at intermediate times. As highlighted by the arrow in Figure 3, the systems with high N exhibit a common plateau value or an inflection point at a similar ϕ value. On the other hand, for polymers with $N < 35$ the inflection point of the curves appears at lower ϕ values. This displays in a model independent way that $\Delta\epsilon_{\text{NM}}/\Delta\epsilon_\alpha$ stays constant for high N , as is to be expected in the Gaussian regime, according to the following argument: With N_{NM} denoting the number of polymer chains per volume and μ_{NM}^2 their mean-square end-to-end dipole moment, at a given temperature one has

$$\Delta\epsilon_{\text{NM}} \propto \frac{N_{\text{NM}}}{V} \mu_{\text{NM}}^2 = \frac{N_s}{N_{\text{s/pol}}} \frac{1}{V} \mu_{\text{NM}}^2 \quad (1)$$

Here we expressed N_{NM} by the total number of segments, N_s , and by the number of segments per chain, $N_{\text{s/pol}}$. For a Gaussian

*Corresponding author. E-mail: catalin.gainaru@uni-dortmund.de.

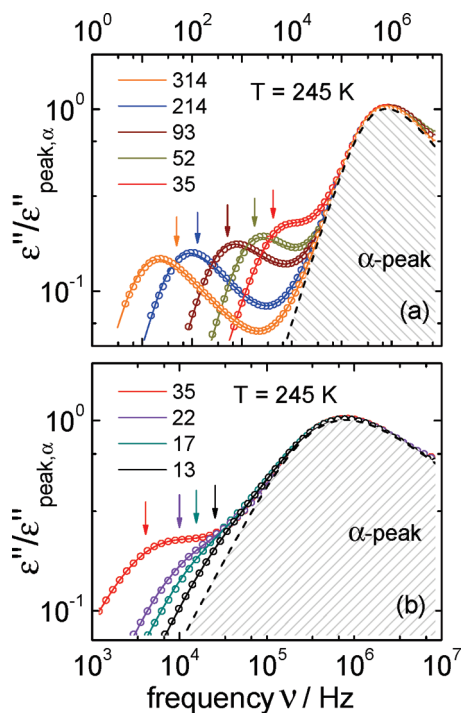


Figure 1. Dielectric spectra for all polymers at $T = 245$ K. The amplitude of the data is normalized by the maximum of the α -peak. For clarity, the data are presented in frames (a) for $N \geq 35$ and (b) for $N \leq 35$ with different frequency scales. Solid lines are fits with the Havriliak–Negami functions as described in the text. The dashed lines mark the area of the α -peak contribution (with $\alpha_\alpha = 0.88$).

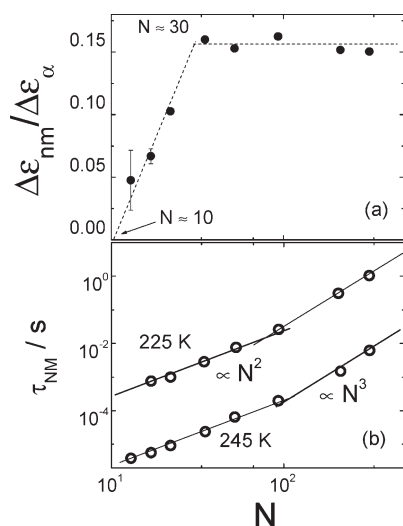


Figure 2. (a) Relative dielectric strengths of the NM with respect to that of the α -peak as a function of the number N of repeat units. The dashed lines are guides for the eye. (b) NM relaxation times at two temperatures. The solid lines are power-laws with exponents 2 and 3. These are not the result of fits but drawn to highlight the molecular weight (or the number of repeat units N), beyond which, due to entanglements effects, the Rouse theory is no longer applicable.

chain one has $\mu_{NM}^2 = N_{s/pol} \mu_s^2$. Combination with eq 1 yields

$$\Delta\epsilon_{NM} \propto \frac{N_s}{V} \mu_s^2 \propto \Delta\epsilon_\alpha \quad (2)$$

Thus, the ratio of $\Delta\epsilon_{NM}$ and $\Delta\epsilon_\alpha$ is independent of N ; in other words, eq 2 provides a clear-cut criterion to recognize the onset of the Gaussian behavior from the static properties of polymer

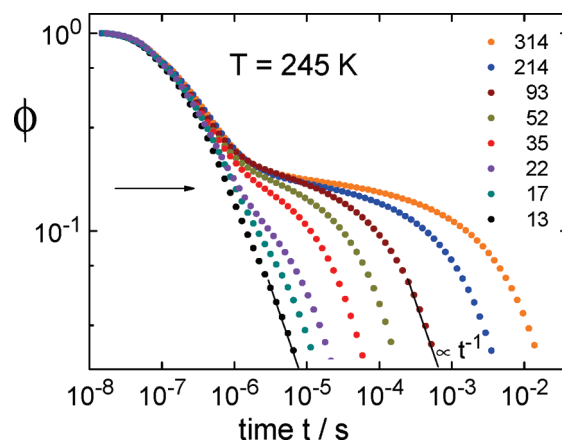


Figure 3. Step response functions calculated from the spectra in Figure 1. The arrow highlight the N -independent relative strength of the NM with respect to the α -process for $N > 35$ as indicated by the horizontal dashed line in Figure 2a. The solid lines indicate a terminal exponential decay.

chains. Furthermore, eq 2 is in marked contrast to the widespread, conventional contention^{11,19} that $\Delta\epsilon$ can be used to measure the chain's end-to-end distance in the Gaussian regime. This contention is the more surprising since even some classical data on polyisoprene imply such an N independence of $\Delta\epsilon_{NM}/\Delta\epsilon_\alpha$ which, however, was not commented by the authors of ref 11.

Not only the amplitude but also the time scales exhibit interesting scaling behaviors. On the one hand, the segmental relaxation time of all the investigated systems is essentially independent of N and thus not suitable for a clear-cut distinction of dynamical regimes. On the other hand, the normal mode more rapidly slows down with increasing M_w . Figure 2b summarizes the molecular weight dependence of τ_{NM} at two temperatures. In each case τ_{NM} follows a power law, $\propto N^a$, with the exponent changing from $a = 2$ to $a \approx 3$. It is clear from the data shown in Figure 2b that the larger exponent cannot be determined precisely. Previous measurements reported slightly different value for a in a more limited M_w range.¹⁹ The change of slope obvious from Figure 2b indicates an entanglement molecular weight, $M_e \approx 5300$ g/mol, corresponding to $N_e = 90$, in rough agreement with previous estimates which gave $M_e \approx 7000$ g/mol.²⁰ Slightly smaller M_e values were obtained via NMR diffusion techniques, pointing to the existence of transient entanglements for this polymer.²¹

While it is thus well established up to which N the Rouse regime extends, the low- N limit of this range is not yet clear. To address this question, we have to go beyond analyzing the mean time scales of the fundamental Rouse modes and to take the entire shape of the dielectric loss spectrum into account. According to the Rouse model, this is achieved by carrying out the Fourier transform of the correlation function

$$\langle \vec{R}_{NM}(0) \vec{R}_{NM}(t) \rangle \propto N \sum_{\substack{k=1 \\ \text{odd}}}^N \frac{1}{k^2} \exp(-t/\tau_k) \quad (3)$$

which involves a rapidly converging sum. With ζ and γ denoting monomeric friction coefficient and effective spring constant, respectively, the time scale of the k th order Rouse mode is

$$\tau_k = \frac{\gamma}{\zeta} 4 \sin^{-2} \left(\frac{k\pi}{2N} \right) \quad (4)$$

Hence, while according to eq 3 the shape of the Rouse mode involves no adjustable parameters, its entire spectrum of time

constants via eq 4 is fixed by specifying *one* single time scale, e.g., the highest-order Rouse mode τ_N corresponding to a single Rouse bead.

The NM peak positions for the dominating $k = 1$ mode, calculated based on eqs 3 and 4, are indicated by the arrows in Figure 1. They agree with the experimental data, except for large $M_w > M_e$ (or $N > 90$). Here reptation effects are expected to come into play. For the calculations we used the same τ_N for all N , and for simplicity we choose $\tau_N = \tau_\alpha$. This choice does not mean that the Rouse bead should be identified with the monomer unit since $\tau_k/\tau_j \approx (M_k/M_j)^2$, and hence a different supramolecular subunit could have been chosen. This implies that information about the length of the Kuhn segment, as an example of such a subunit, cannot be inferred directly from the present analysis.

Returning to the comparison of the Rouse calculations with the experimental NM loss maxima shown in Figure 1, it is remarkable that good agreement is obtained down to $N = 13$. This is significantly smaller than the number of monomer units above which the chain is Gaussian, based on the criterion formulated with the help of Figure 2a.

To summarize, the change from the Gaussian to non-Gaussian polymer behavior is displayed in a clear-cut fashion via the N independence of the static susceptibility of the dielectric normal mode relative to that of the segmental mode. However, for PPG, this transition is not obvious from the analysis of time scales, i.e., from dynamic variables. These results cannot be easily understood within the Rouse theory. The latter assumes entropic properties of the Kuhn segment, a condition which is not satisfied for a non-Gaussian chain.

References and Notes

- (1) Doi, M.; Edwards, S. F. *The Theory of Polymer Dynamics*; Clarendon: Oxford, 1986. de Gennes, P. G. *Scaling Concepts in Polymer Physics*; Cornell University Press: New York, 1979.
- (2) Baur, M. E.; Stockmayer, H. *J. Chem. Phys.* **1965**, *43*, 4319.
- (3) Beevers, M. S.; Elliott, D. A.; Williams, G. *Polymer* **1980**, *21*, 13.
- (4) Adachi, K.; Kotaka, T. *Macromolecules* **1987**, *20*, 2018.
- (5) Jacobsson, P.; Börjesson, L.; Torell, L. M. *J. Non-Cryst. Solids* **1991**, *131–133*, 104.
- (6) Ding, Y.; Kisliuk, A.; Sokolov, A. P. *Macromolecules* **2004**, *37*, 161.
- (7) Kariyo, S.; Gainaru, C.; Schick, H.; Brodin, A.; Rössler, E. A. *Phys. Rev. Lett.* **2006**, *97*, 207803.
- (8) Paul, W. *Chem. Phys.* **2002**, *284*, 59 and references cited therein.
- (9) Hintermeyer, J.; Herrmann, A.; Kahlau, R.; Goiceanu, C.; Rössler, E. A. *Macromolecules* **2008**, *41*, 9335.
- (10) Agapov, A. L.; Sokolov, A. P. *Macromolecules* **2009**, *42*, 2877.
- (11) Adachi, K.; Kotaka, T. *Prog. Polym. Sci.* **1993**, *18*, 585.
- (12) Boese, D.; Kremer, F. *Macromolecules* **1990**, *23*, 829.
- (13) Mattsson, J.; Bergman, R.; Jacobsson, P.; Börjesson, L. *Phys. Rev. Lett.* **2005**, *94*, 165701. Leon, C.; Ngai, K. L.; Roland, C. M. *J. Chem. Phys.* **1999**, *110*, 585. Grzybowska, K.; Grzybowski, A.; Ziolo, J.; Rzoska, S. J.; Paluch, M. *J. Phys.: Condens. Matter* **2007**, *19*, 376105. Köhler, M.; Lunkenheimer, P.; Goncharov, Y.; Wehn, R.; Loidl, A. **2008**, arXiv:0810.5316v1.
- (14) Samples with the number of repeat units N given in brackets were from PSS Mainz ($N = 13, 17, 35, 52, 93$) and Bayer Co. ($N = 214, 314$). Additionally, a sample with $N = 22$ was kindly provided by Dr. A. Schönhals.
- (15) Osaki, S.; Uemura, S.; Ishida, Y. *J. Polym. Sci.* **1971**, *A-2*, 9585. Nazemi, A.; Williams, G.; Attard, G. S.; Karasz, F. E. *Polym. Adv. Technol.* **1992**, *3*, 157 and references cited therein.
- (16) A dc bias of 20 V was applied to the samples at room temperature so that mobile charges can accumulate at the electrodes. After about 2 h the samples were cooled with the bias still on. Further details will be given in C. Gainaru and R. Böhmer (to be published).
- (17) Moon, I. K.; Jeong, Y. H.; Furukawa, T. *Thermochim. Acta* **2001**, *377*, 97.
- (18) Williams, G.; Watts, D. C. *Trans. Faraday Soc* **1971**, *67*, 1971.
- (19) Schönhals, A. In *Broadband Dielectric Spectroscopy*; Kremer, F., Schönhals, A., Eds.; Springer: Berlin, 2003; Chapter 7.
- (20) Smith, B. A.; Samulski, E. T.; Winnik, M. A. *Macromolecules* **1985**, *18*, 1901.
- (21) Appel, M.; Fleischer, G.; Kärger, J.; Chang, I.; Fujara, F.; Schönhals, A. *Colloid Polym. Sci.* **1997**, *275*, 187.